RESEARCH ARTICLE

Figures and figure supplements

Dual midbrain and forebrain origins of thalamic inhibitory interneurons

Polona Jager *et al*

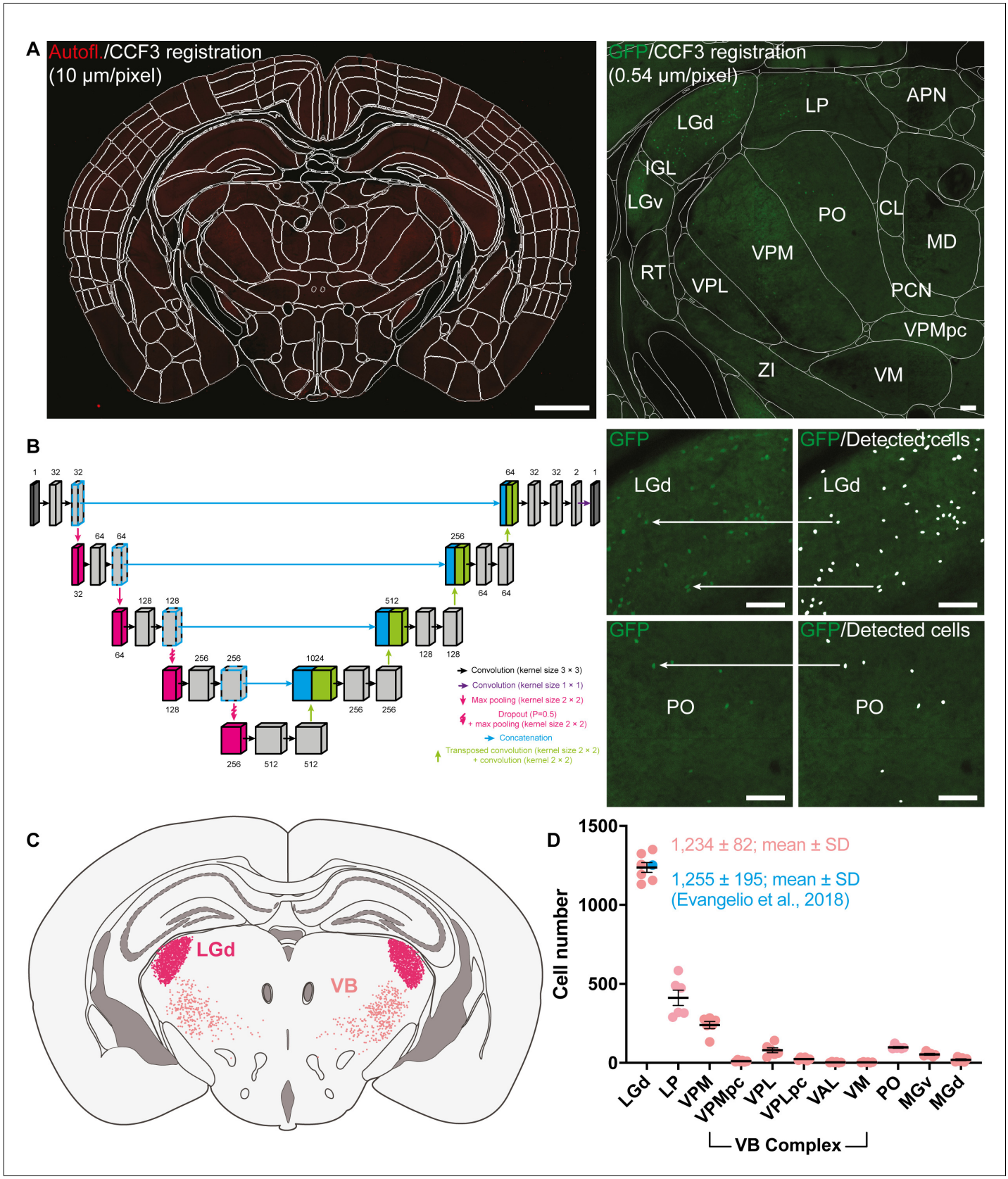

Figure 1. Automated total counts of GFP^{+} cells in the thalamus of the *Sox14*$^{GFP/+}$ mouse. (**A**) Autofluorescence (Autofl.) from serial two-photon imaging of Sox14$^{GFP/+}$ mice (n = 3) at 0.54 × 0.54 × 10 µm voxel resolution was registered to the Allen Institute CCF3 atlas using Elastix (left; scale bar 1 mm).

Figure 1 continued on next page

Figure 1 continued

This permits delineation and identification of all anatomical structures according to the Allen Institute hierarchical taxonomy (right; scale bar 100 μm). (**B**) Automated cell detection was done using a U-Net trained on 219 manually segmented images (512 × 512 pixels) augmented to a total sample size of 12,264, split 75% for training and 25% validation. Images containing GFP fluorescence were passed into the trained U-Net (left) for cell prediction based on learned features during training (right; scale bar 100 μm). Oversampling in the z-axis was corrected for by grouping and averaging detected cell positions which colocalised within a defined cell radius. (**C**) Example illustration of automatically detected cells in the LGd and VB complex projected onto a representative coronal section of the thalamus. (**D**) Quantification of GFP^+ cells in the LGd at 1234 ± 82 (mean ± SD) validated against stereological study by ***Evangelio et al., 2018*** of 1255 ± 195 (mean ± SD) interneurons in the LGd. Other counts are shown for LP, VB complex [VPM, parvicellular part of the ventral posteromedial nucleus (VPMpc), VPL, parvicellular part of the ventral posterolateral nucleus (VPLpc), VAL, VM], MGv, MGd, and PO.

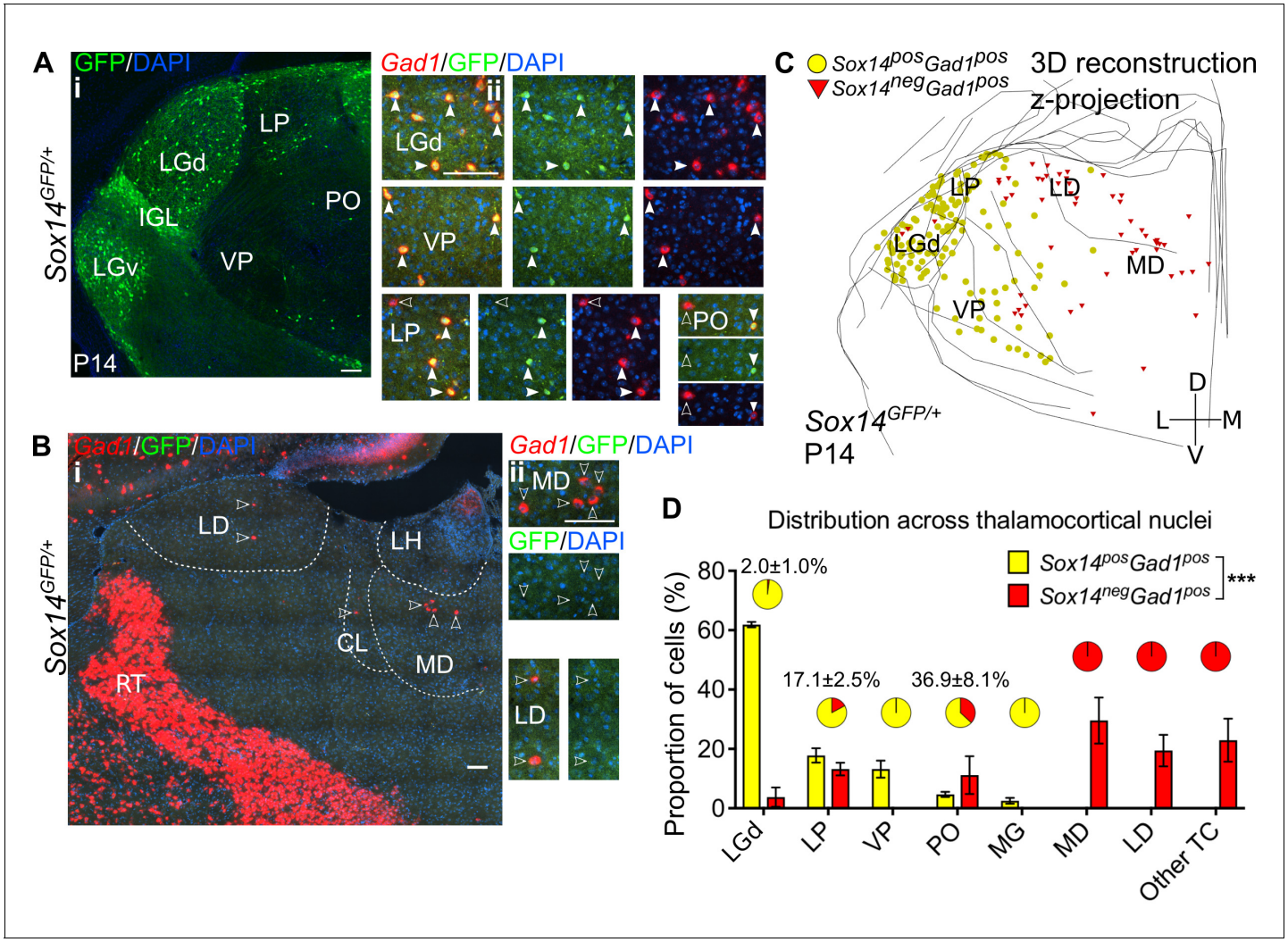

Figure 2. Diversity and distribution of GABAergic cells in the mouse thalamocortical nuclei. (**A**) (i) Representative coronal section of P14 *Sox14*$^{GFP/+}$ thalamus with *Sox14*$^{+}$ cells in the LGd, VP, LP, and PO. (ii) *Sox14*$^{+}$ cells in TC regions co-express *Gad1*, but not all *Gad1*$^{+}$ cells co-express *Sox14* in the LP and PO. Filled arrows mark *Sox14*$^{+}$*Gad1*$^{+}$ and empty arrows *Sox14*$^{-}$*Gad1*$^{+}$ cells. Scale bars, 100 µm. (**B**) (i) Representative rostral coronal section of P14 *Sox14*$^{GFP/+}$ thalamus with *Gad1*$^{+}$ cells in the MD, CL, and LD, which contain no *Sox14*$^{+}$ cells. (ii) *Gad1*$^{+}$ cells in these nuclei do not co-express *Sox14*. Scale bars, 100 µm. (**C**) 3D reconstruction of a representative P14 *Sox14*$^{GFP/+}$ thalamus from tracing every tenth 20-µm-thick coronal section, displayed as a z-projection and showing distribution of *Sox14*$^{+}$*Gad1*$^{+}$ (yellow) and *Sox14*$^{-}$*Gad1*$^{+}$ cells (red). One dot represents one neuron. (**D**) Distribution of *Sox14*$^{+}$*Gad1*$^{+}$ and *Sox14*$^{-}$*Gad1*$^{+}$ cells across TC nuclei in the *Sox14*$^{GFP/+}$ brains at P14, plotted as proportion of all the cells within each interneuron group (mean ± SEM; n = 3 brains). The category 'other TC' refers to regions where nuclear boundaries cannot be defined precisely and that contain VAL, VM, CL, IMD, PF, RE, RH, SPF, SPA, CM, and AM. *Sox14*$^{+}$*Gad1*$^{+}$ and *Sox14*$^{-}$*Gad1*$^{+}$ populations have distinct distributions ($p<10^{-3}$ chi-squared test). Pie charts show the proportion (mean ± SEM) of the two interneuron classes within each nucleus.

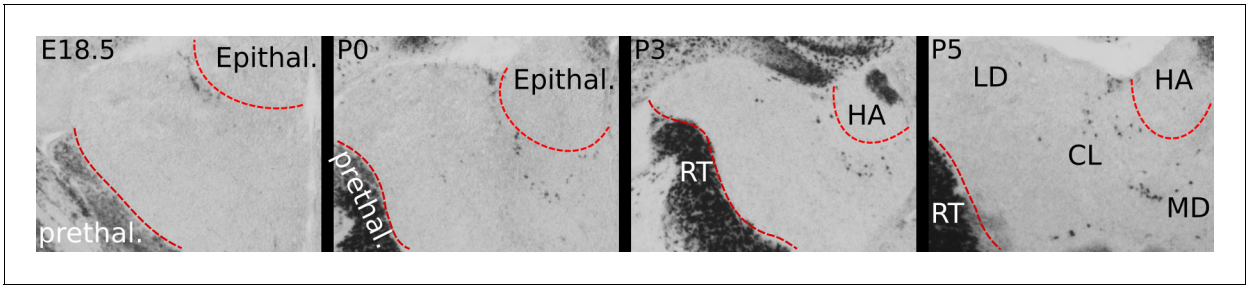

Figure 2—figure supplement 1. Perinatal distribution of *Gad1*$^{+}$ cells in the anterior thalamus. Before birth, *Gad1*$^{+}$ cells are not present within rostral thalamic tissue that harbours HO nuclei including the LD, CL, and MD. By E18.5, a cluster of *Gad1*$^{+}$ cells is present at the outer edge of the thalamus, bordering the epithalamus. From this location, *Gad1*$^{+}$ cells appear to spread medially first, following the contour of the ventral edge of the habenula (HA), part of the epithalamus. At P0 and during the following 4 days, *Gad1*$^{+}$ cells appear to penetrate thalamic tissue and to scatter in the LD, CL, and MD.

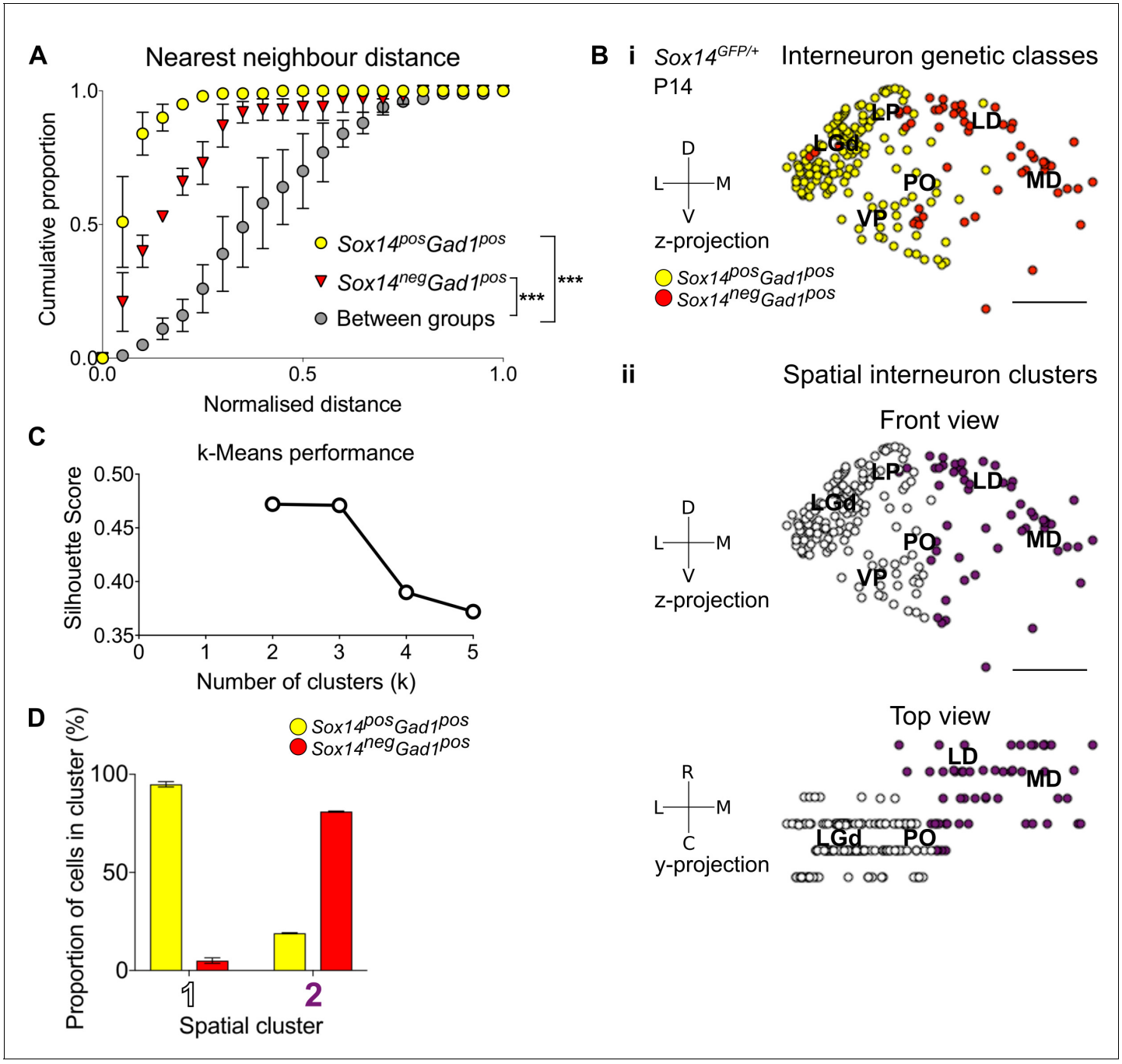

Figure 3. Spatial organisation of thalamic GABAergic cells. (**A**) Normalised nearest neighbour distance (NND) for *Sox14*$^{+}$*Gad1*$^{+}$ and *Sox14*$^{-}$*Gad1*$^{+}$ populations and between the two groups from P14 *Sox14*$^{GFP/+}$ data (***Figure 2***), plotted as cumulative proportion of all cells within a given set. The NND distribution is significantly shifted to larger distances between groups than within each of the groups ($p<1.4 \times 10^{-30}$, two-sample Kolmogorov–Smirnov test, n = 3 brains). (**B**) Representative z-projections of interneuron distribution amongst TC nuclei, from P14 *Sox14*$^{GFP/+}$ data (***Figure 2***). One dot represents one neuron and they are colour coded by (i) their genetic identity or (ii) spatial cluster. For the spatial clusters a y-projection is also shown. Scale bars, 500 µm. (**C**) Performance of unsupervised k-means algorithm in identifying thalamic interneuron spatial clusters from the P14 *Sox14*$^{GFP/+}$ data (n = 3 brains, see also ***Figure 2***) as measured by the silhouette score, which varies with number of clusters (k). We choose k = 2 as this point has the highest score. (**D**) Proportion of *Sox14*$^{+}$ and *Sox14*$^{-}$ GABAergic cells in each spatial cluster, averaged over three brains (mean ± SEM).

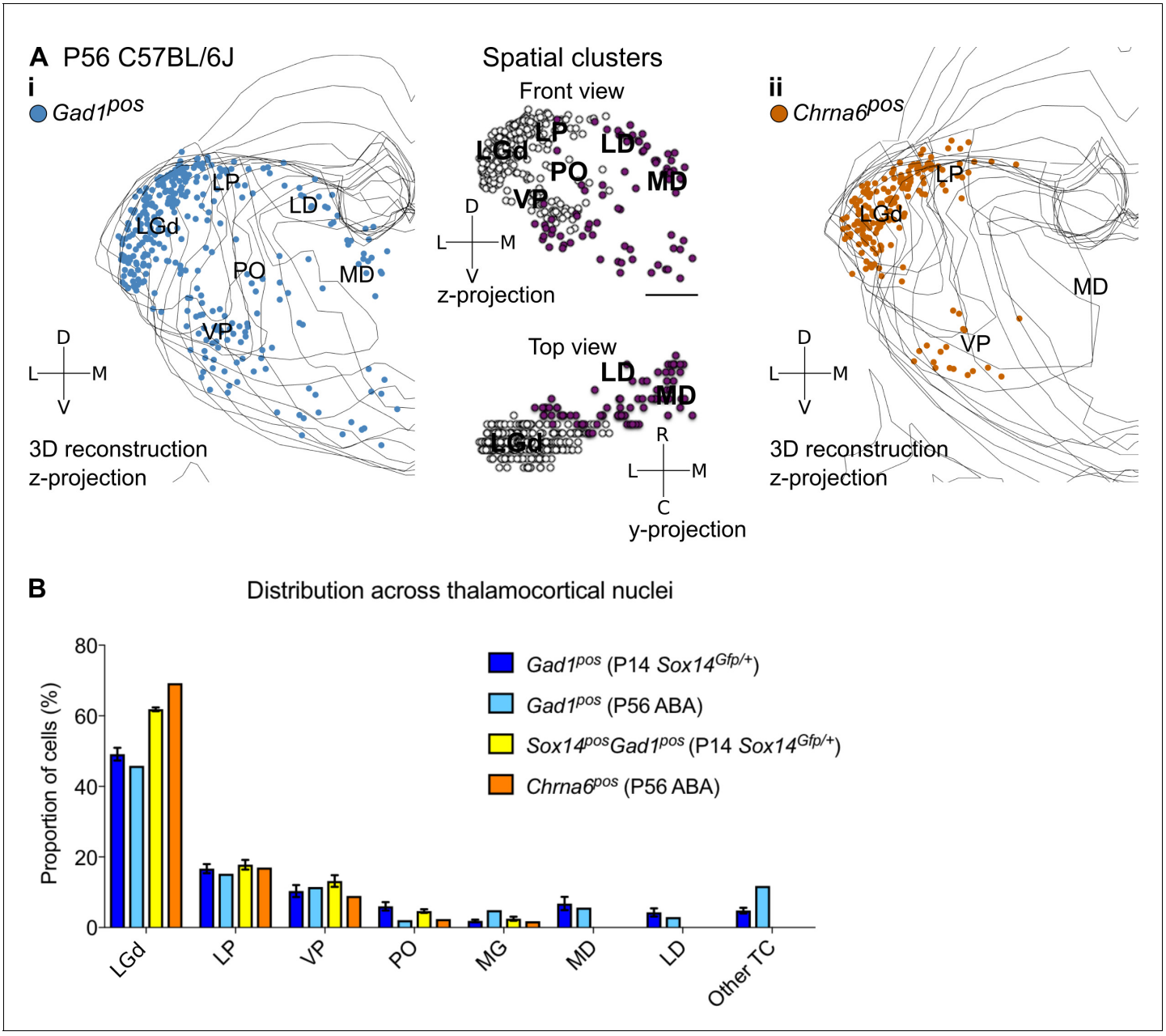

Figure 3—figure supplement 1. Spatial organisation of *Gad1*$^{+}$ and *Chrna6*$^{+}$ cells in the adult mouse thalamus. (**A**) 3D reconstruction of a representative P56 mouse thalamus from tracing every eight 25-µm-thick coronal section, displayed as a z-projection and showing distribution of (i) *Gad1*$^{+}$ and (ii) *Chrna6*$^{+}$ cells. In (i), k-means clustering was applied to the data using k = 2 (highest silhouette score, 0.512); the resulting spatial clusters are shown as a z- and y-projection and colour coded. One dot represents one neuron. ISH data was downloaded from the Allen Mouse Brain Atlas (2004 Allen Institute for Brain Science. Allen Mouse Brain Atlas. Available from: mouse.brain-map.org; ***Lein et al., 2007***). (**B**) Distribution of *Gad1*$^{+}$ and *Chrna6*$^{+}$ cells across TC nuclei (n = 1 brain/marker) is compared to all *Gad1*$^{+}$ and *Sox14*$^{+}$*Gad1*$^{+}$ cells from P14 *Sox14*$^{GFP/+}$ thalamus (n = 3 brains; see also ***Figure 2***).

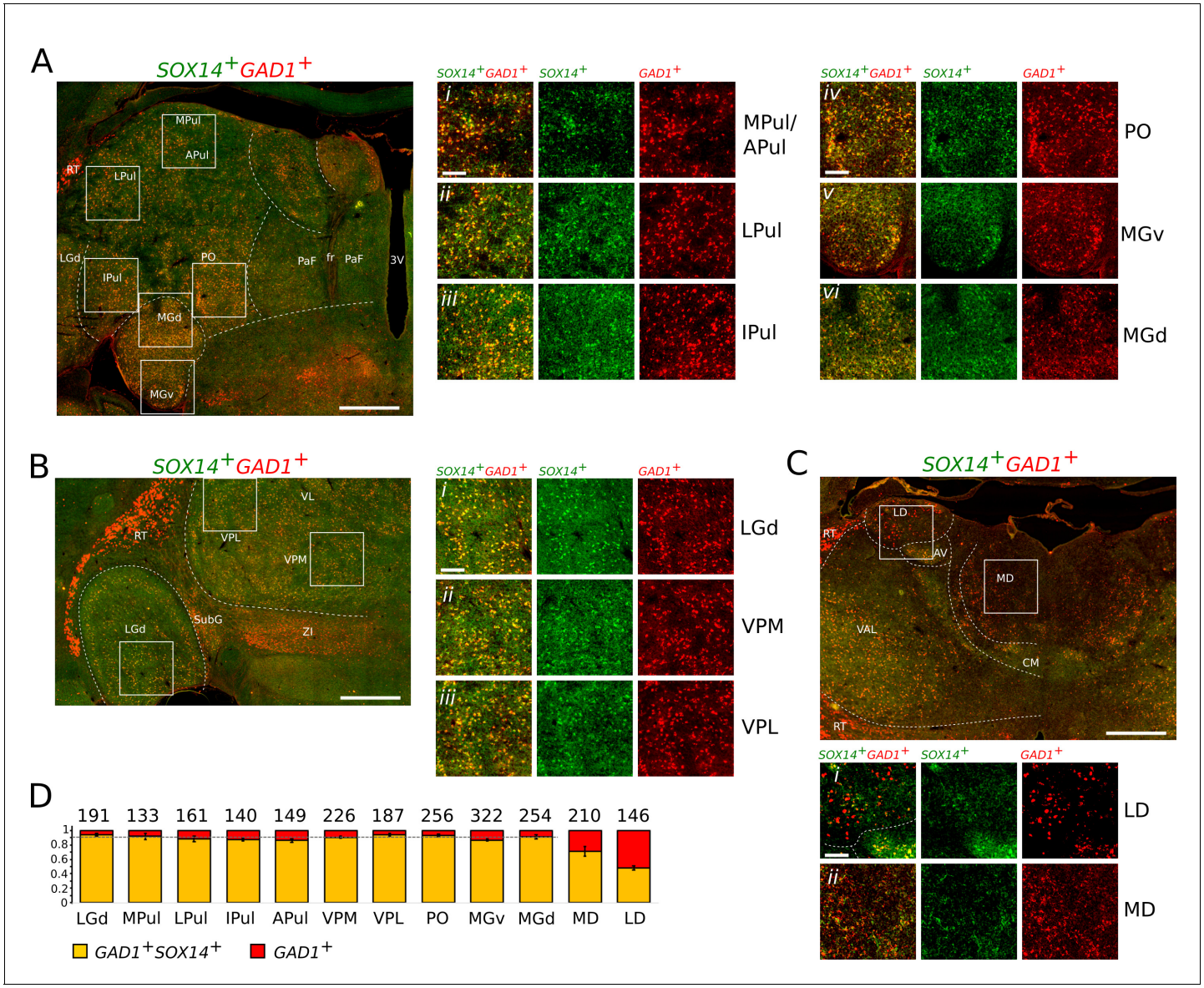

Figure 4. *SOX14*$^{+}$*GAD1*$^{+}$ interneurons dominate TC regions of the non-human primate marmoset. Representative coronal sections of the thalamus of a new-born marmoset illustrating the distribution of cells expressing the *SOX14* (green) and *GAD1* (red) mRNAs. (**A**) Caudal plane containing subdivisions of the pulvinar complex, the PO, and the auditory MG. Also visible are parafascicular (PaF) nuclei. Fr, fasciculus retroflexus; 3V, third ventricle. (Ai–iii) Magnifications of indicative areas of the medial (MPul) and anterior pulvinar (APul), the lateral pulvinar (LPul), and inferior pulvinar (IPul). (Aiv). Magnification of a region of the PO. (Av and vi). Magnifications of representative regions of the ventral (MGv) and dorsal (MGd) subdivisions of the auditory thalamus. (**B**) Middle plane section containing the sensory TC nuclei LGd, VPM, VPL, and other non-TC structures (ZI, RT, and SubG). (Bi–iii). Magnifications illustrating the dominant presence of *SOX14*$^{+}$*GAD1*$^{+}$ interneurons in the sensory FO nuclei. (**C**) Anterior plane containing the VAL, centromedial (CM), anteroventral (AV), LD, and MD. The prethalamic RT is recognisable as an entirely *SOX14*$^{-}$*GAD1*$^{+}$ structure. (Ci). Magnification of an area of the LD containing comparable densities of *SOX14*$^{+}$ and *SOX14*$^{-}$ interneurons. (Cii). Magnification of an area of the MD containing *SOX14*$^{+}$ and *SOX14*$^{-}$ interneurons. (**D**) Fraction of *SOX14*$^{+}$*GAD1*$^{+}$ (yellow) and *SOX14*$^{-}$*GAD1*$^{+}$ (red) interneurons in selected TC nuclei. Above each bar the total cell counts from nine regions of interest (ROI) measuring 263 µm by 263 µm per each TC nucleus in three age-matched brains (three ROI per TC nucleus per brain). The average fraction of *SOX14*$^{-}$*GAD1*$^{+}$ interneurons deviates significantly from background level in the MD and LD. Scale bars: low magnification; overviews: ~1 mm; magnified areas:~0.2 mm.

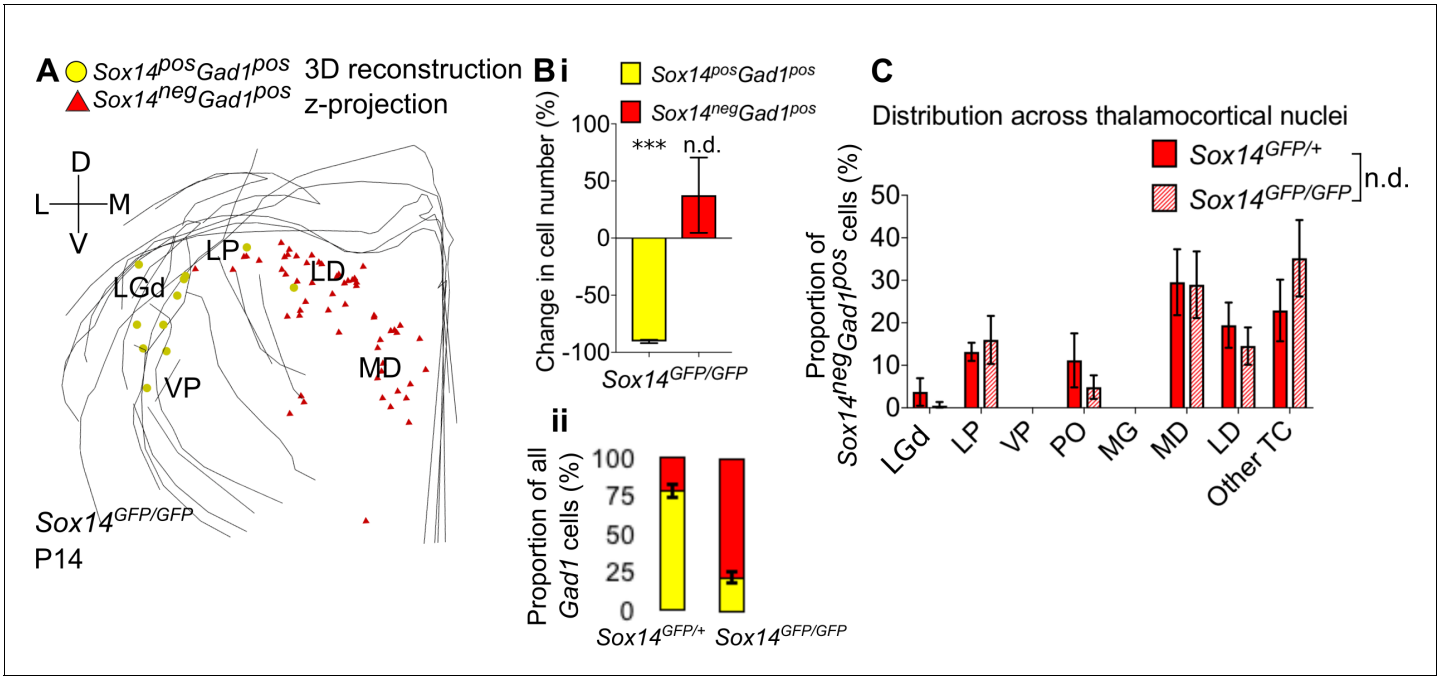

Figure 5. Differential requirement for Sox14 highlights two distinct developmental classes. (**A**) Differential requirement for Sox14 highlights two distinct developmental classes. 3D reconstruction of a representative P14 *Sox14*$^{GFP/GFP}$ thalamus from tracing every tenth 20-µm-thick coronal section, displayed as a z-projection and showing distribution of *Sox14*$^{+}$*Gad1*$^{+}$ (yellow) and *Sox14*$^{-}$*Gad1*$^{+}$ cells (red). (**B**) (**i**) Relative change in the number of GFP^{+}*Gad1*$^{+}$ and GFP^{-}*Gad1*$^{+}$ cells across TC regions in P14 *Sox14*$^{GFP/GFP}$ relative to P14 *Sox14*$^{GFP/+}$ data (mean ± SEM, n = 3 brains/genotype). There is a significant reduction in the GFP^{+}*Gad1*$^{+}$ population ($p=2.7 \times 10^{-4}$, two-sample two-tailed t-test), but no statistically significant difference in the size of the GFP^{-}*Gad1*$^{+}$ group (p=0.4, two-sample two-tailed t-test). (ii) Proportion of GFP^{+}*Gad1*$^{+}$ cells within the total GABAergic population is decreased in the *Sox14*$^{GFP/GFP}$ (mean ± SEM, n = 3 brains/genotype). (**C**) Distribution of GFP^{-}*Gad1*$^{+}$ cells across TC nuclei in the *Sox14*$^{GFP/+}$ and *Sox14*$^{GFP/GFP}$ brains at P14 (mean ± SEM; n = 3 brains/genotype). GFP^{-}*Gad1*$^{+}$ distribution is unaltered in the *Sox14* KO (p>0.05, chi-squared test).

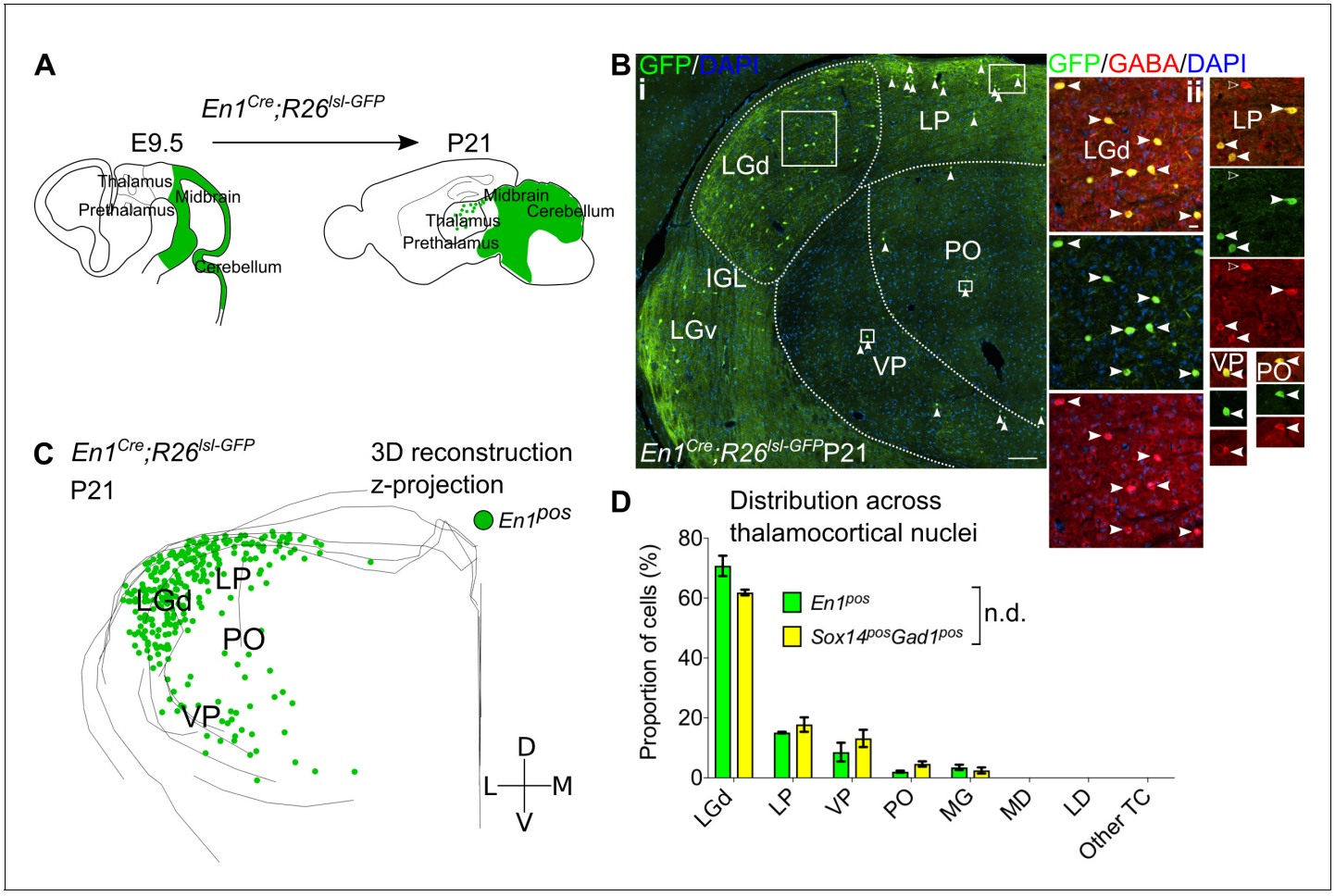

Figure 6. *Sox14*$^{+}$ interneurons in TC regions derive from the midbrain. (**A**) Schematic of the fate mapping experiment: crossing *En1*^{Cre} with *Rosa26*$^{lsl\text{-}GFP}$ reporter line permanently labels all midbrain born cells with GFP expression. (**B**) (i) Representative coronal section of P21 *En1*^{Cre}; *Rosa26*$^{lsl\text{-}GFP}$ thalamus with *En1*$^{+}$ cells observed in the LGd, LP, VP, and PO (considering TC regions only). For clarity some of the *En1*$^{+}$ cells are indicated with white arrows. Scale bar, 100 µm. (ii) *En1*$^{+}$ cells in these regions co-express GABA (filled white arrows). Empty arrows mark GABA single-positive cells. Scale bar, 10 µm. (**C**) 3D reconstruction of a representative P21 *En1*^{Cre}; *Rosa26*$^{lsl\text{-}GFP}$ thalamus from tracing every sixth 60-µm-thick coronal section, displayed as a z-projection and showing distribution of *En1*$^{+}$ cells. (**D**) Distribution of *Sox14*$^{+}$*Gad1*$^{+}$ and *En1*$^{+}$ cells across TC nuclei in *Sox14*$^{GFP/+}$ and *En1*^{Cre}; *Rosa26*$^{lsl\text{-}GFP}$ brains, respectively, plotted as proportion of all the cells within each group (mean ± SEM; n = 3 brains/genotype). The two populations are not differently distributed (p>0.05, chi-squared test).

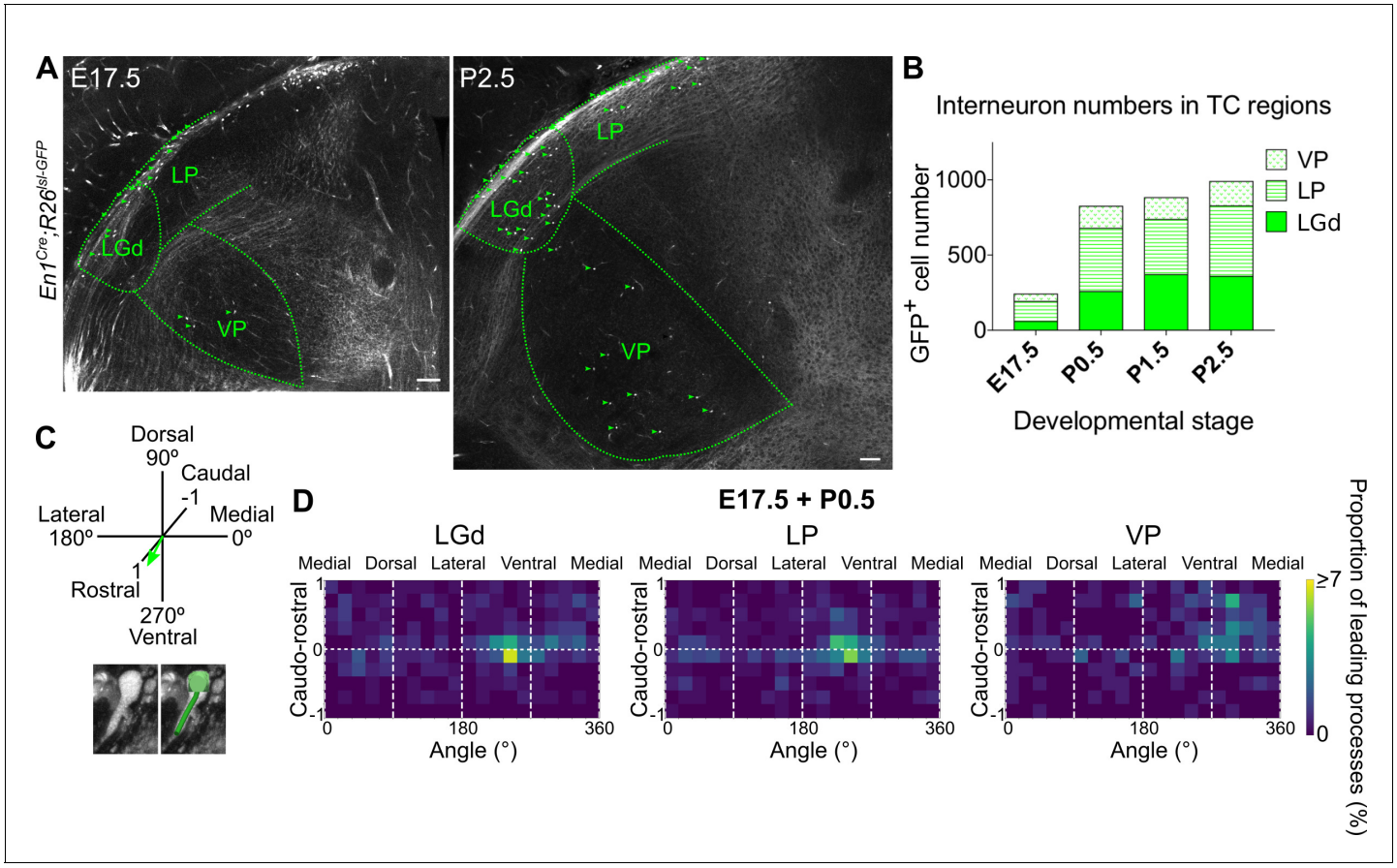

Figure 7. Midbrain-derived interneuron precursors progressively populate the thalamus from E17.5 onwards. (**A**) Representative coronal sections of *En1*^{Cre}; *Rosa26*$^{lsl\text{-}GFP}$ thalamus at E17.5 and P2.5. Green arrows mark some of the GFP^{+} cells. Scale bars, 100 µm. (**B**) Number of GFP^{+} cells counted in the LGd, LP, and VP from E17.5 to P2.5 (mean, n = 3 brains). (**C**) Leading process orientation of GFP^{+} cells was determined along the caudo-rostral, ventro-dorsal, and latero-medial dimensions. (**D**) Frequency distribution of leading process orientation for GFP^{+} cells in the LGd, LP, and VP at E17.5 and P0.5 combined, represented in heat maps (n = 3 brains/developmental stage).

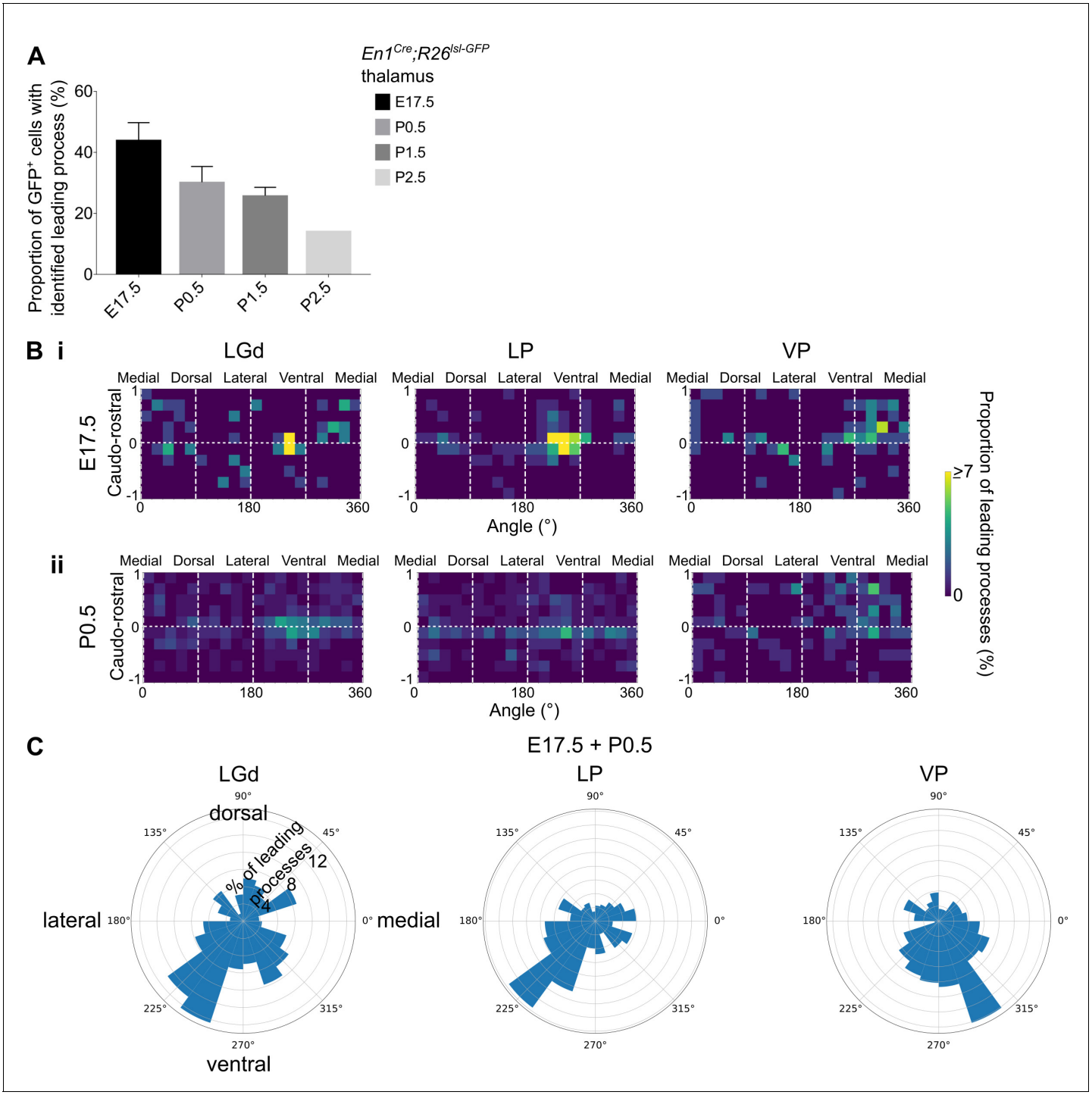

Figure 7—figure supplement 1. Distinct leading process orientation between interneuron precursors in the LGd and LP compared to VP. (**A**) Proportion of GFP$^+$ cells in the LGd, LP, and VP combined, for which a leading process could be identified, in E17.5-P2.5 *En1^{Cre}; Rosa26$^{lsl\text{-}GFP}$* brains (mean ± SEM, n = 3 brains/developmental stage, apart from P2.5 where n = 1 brain). (**B**) Frequency distribution of leading process orientation for GFP$^+$ cells in the LGd, LP, and VP at (i) E17.5 and (ii) P0.5 separately, represented in heat maps (n = 3 brains/developmental stage). (**C**) Polar histograms of leading process orientation in the latero-medial and ventro-dorsal plane for GFP$^+$ cells in the LGd, LP, and VP at E17.5 and P0 combined (n = 3 brains/developmental stage).

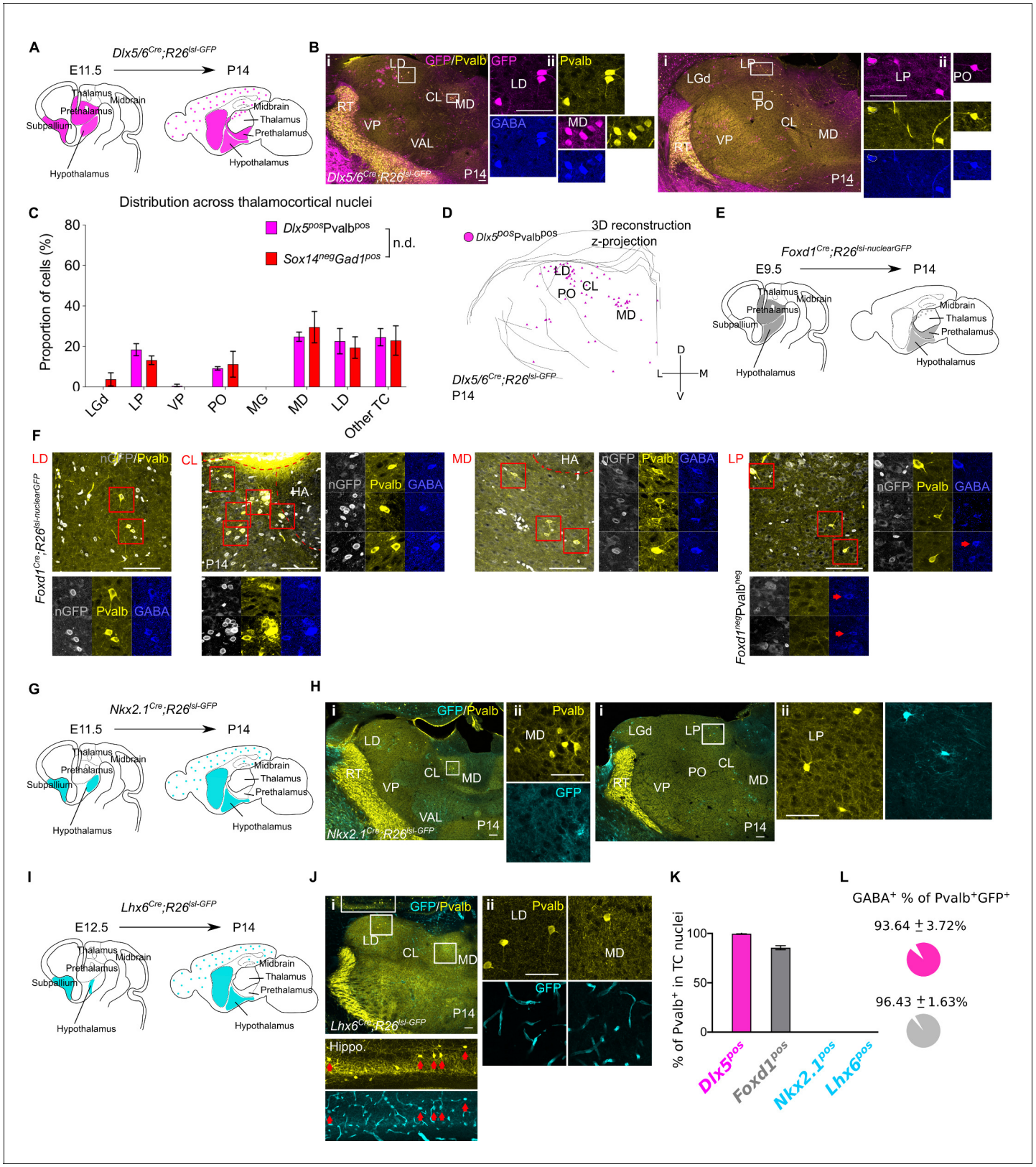

Figure 8. *Sox14*$^{-}$*Pvalb*$^{+}$ interneurons in TC regions derive from the *Dlx5*^{pos}, *Foxd1*^{pos}, *Nkx2.1*^{neg}, *and Lhx6*^{neg} rostral forebrain. (**A**) Schematic of the fate mapping experiment: crossing *Dlx5/6*^{Cre} with *Rosa26*$^{lsl\text{-}GFP}$ reporter line permanently labels all ventral telencephalic, hypothalamic, and prethalamic-born cells with GFP expression. (**B**) (i) Representative coronal sections of P14 *Dlx5/6*^{Cre}; *Rosa26*$^{lsl\text{-}GFP}$ thalamus with *Dlx5*$^{+}$Pvalb^{+} cells present in the MD,

Figure 8 continued on next page

Figure 8 continued

LD, CL, VAL, VM, LP, and PO (considering TC regions only). Scale bar, 100 μm. (ii) *Dlx5*$^{+}$Pvalb^{+} cells in TC regions co-express GABA. Scale bar, 100 μm. (**C**) Distribution of *Dlx5*$^{+}$Pvalb^{+} and *Sox14*$^{-}$*Gad1*$^{+}$ cells across TC nuclei in P14 *Dlx5/6*^{Cre}; *Rosa26*$^{lsl\text{-}GFP}$ and *Sox14*$^{GFP/+}$ brains, respectively, plotted as proportion of all the cells within each group (mean ± SEM, n = 3 brains/genotype). The two populations are not differently distributed ($p>0.05$, chi-squared test). (**D**) 3D reconstruction of a representative P14 *Dlx5/6*^{Cre}; *Rosa26*$^{lsl\text{-}GFP}$ thalamus from tracing every sixth 60-μm-thick coronal section, displayed as a z-projection and showing distribution of *Dlx5*$^{+}$Pvalb^{+} cells. (**E**) Schematic of the fate mapping experiment crossing the *Foxd1*^{Cre} with *Rosa26*$^{lsl\text{-}nuclearGFP}$ reporter line to permanently label hypothalamic and prethalamic-born cells with nuclear membrane localised GFP. (**F**) Representative coronal sections of P14 *Foxd1*^{Cre}; *Rosa26*$^{lsl\text{-}nuclearGFP}$ thalamus with *Foxd1*$^{+}$Pvalb^{+} cells present in the LD, CL, MD, and LP. Scale bar, 100 μm. Enlarged areas (red boxes) showing *Foxd1*$^{+}$Pvalb^{+} cells co-expressing GABA. Additional GABA^{+} but *Foxd1*$^{-}$Pvalb^{-} neurons are also visible in the LP (red arrows). HA: habenula. (**G**) Schematic of the fate mapping experiment: crossing *Nkx2.1*^{Cre} with *Rosa26*$^{lsl\text{-}GFP}$ reporter line permanently labels some hypothalamic and all MGE-born cells with GFP expression. (**H**) (**i**) Representative coronal sections of P14 *Nkx2.1*^{Cre}; *Rosa26*$^{lsl\text{-}GFP}$ thalamus with Pvalb^{+} and *Nkx2.1*$^{+}$ cells present in the MD, LD, CL, VAL, VM, LP, and PO (considering TC regions only). Scale bar, 100 μm. (ii) *Nkx2.1*$^{+}$ cells in TC regions do not co-express Pvalb^{+}. Scale bar, 100 μm. (**I**).Schematic of the fate mapping experiment crossing the *Lhx6*^{Cre} with *Rosa26*$^{lsl\text{-}GFP}$ reporter line to permanently label some hypothalamic and MGE born cells with GFP. (**J**) (**i**) Representative coronal section of P14 *Lhx6*^{Cre}; *Rosa26*$^{lsl\text{-}GFP}$ showing GFP^{+}Pvalb^{+} cells in the hippocampus (red arrows) and GFP^{-}Pvalb^{+} present in the MD, LD, and CL nuclei of the thalamus (considering TC regions only). Scale bar, 100 μm. (ii) GFP^{+} cells in TC regions are endothelial and do not co-express Pvalb^{+}. Scale bar, 100 μm. (**K**) Proportion of Pvalb^{+} cells in TC regions that are *Dlx5*$^{+}$, *Foxd1*$^{+}$, *Nkx2.1*$^{+}$, or *Lhx6*$^{+}$ at P14 (mean ± SEM, *Dlx5*$^{+}$ n = 3 brains, *Foxd1*$^{+}$ n = 5 brains, *Nkx2.1*$^{+}$ n = 3 brains, and *Lhx6*$^{+}$ n = 4 brains). (**L**) Proportion of *Dlx5*$^{+}$Pvalb^{+} and *Foxd1*$^{+}$Pvalb^{+} cells in TC regions co-expressing GABA at P14 (mean ± SEM, *Dlx5*$^{+}$ n = 3 brains, *Foxd1*$^{+}$ n = 5 brains).

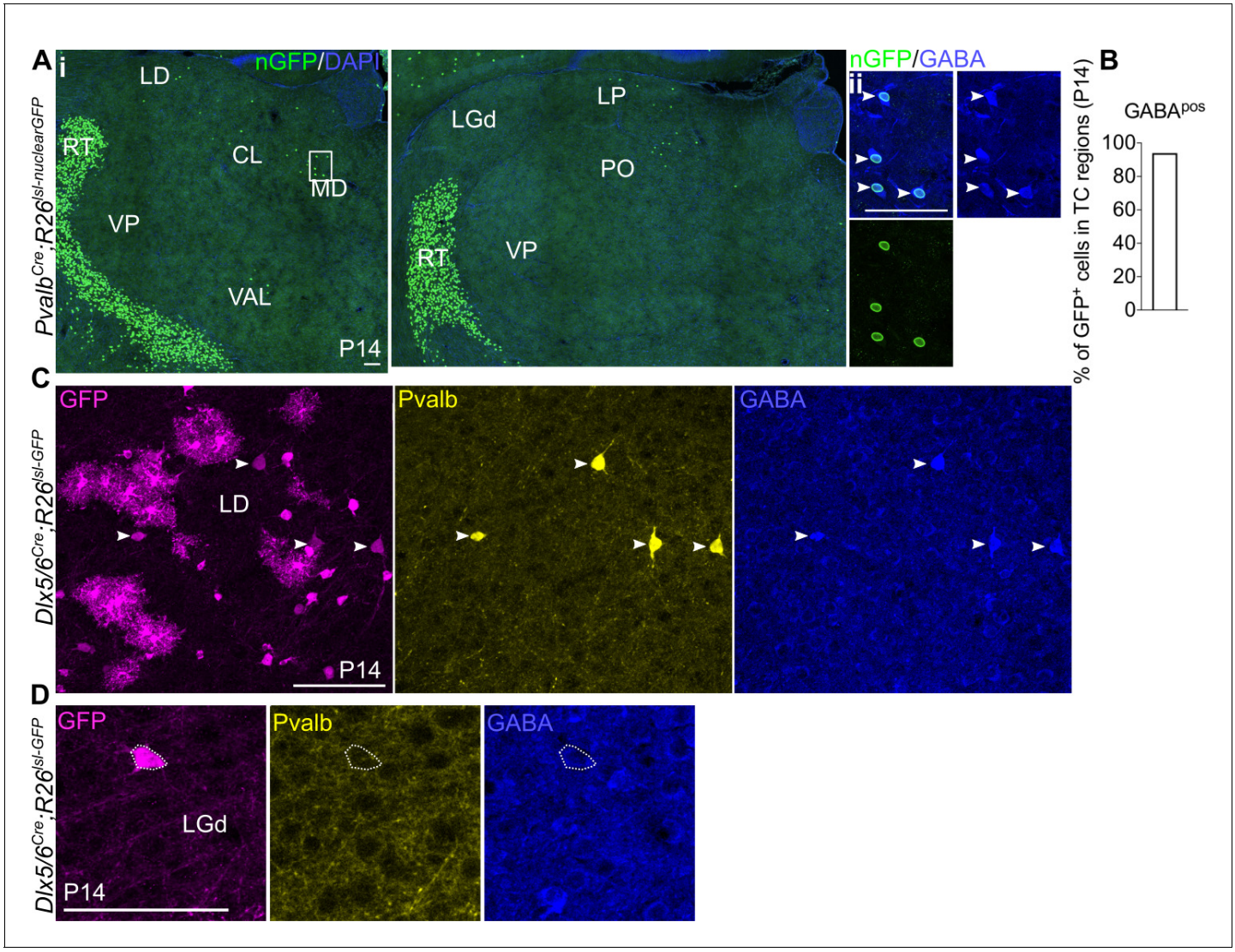

Figure 8—figure supplement 1. Pvalb is a marker for *Sox14*$^-$ thalamic interneurons. (**A**) (i) Representative coronal sections of P14 *Pvalb*^{Cre}; *Rosa26*$^{lsl\text{-}nuclearGFP}$ thalamus with GFP$^+$ cells present in the MD, LD, CL, VAL, LP, and PO (considering TC regions only). Scale bar, 100 µm. (ii) GFP$^+$ cells in TC regions express GABA at P14. Scale bar, 100 µm. (**B**) Proportion of GFP$^+$ cells in TC regions co-expressing GABA at P14 (mean, n = 2 brains). (**C**) Clusters of Pvalb$^-$GABA$^-$*Dlx5*$^+$ glia-like cells are observed across TC regions in the *Dlx5/6*^{Cre}; *Rosa26*$^{lsl\text{-}GFP}$ line at P14, as shown for the LD. White arrows mark Pvalb$^+$GABA$^+$*Dlx5*$^+$ cells. Scale bar, 100 µm. (**D**) Pvalb$^-$*Dlx5*$^+$ cells with neuronal morphology do not express GABA. Scale bar, 100 µm.